

A non-magnetic mechanism of backscattering in helical edge states

I.V. Krainov,^{1,*} R.A. Niyazov,^{1,2} D.N. Aristov,^{1,2,3} and V.Y. Kachorovskii¹

¹*Ioffe Institute, St. Petersburg 194021, Russia*

²*NRC “Kurchatov Institute”, Petersburg Nuclear Physics Institute, Gatchina 188300, Russia*

³*Department of Physics, St. Petersburg State University, St. Petersburg 199034, Russia*

(Dated: December 5, 2025)

We study interaction-induced backscattering mechanism for helical edge states of a two-dimensional topological insulator which is tunnel-coupled to a puddle located near the edge channel. The mechanism does not involve inelastic scattering and is due to the zero-mode fluctuations in a puddle. We discuss in detail a simple model of a puddle — a cavity in the bulk of the topological insulator. Such a cavity also has helical edge states with tunneling coupling to helical states encompassing the topological insulator. We analyze effect of the edge current in the puddle. Although averaged value of this current is equal to zero, its zero-mode fluctuations act, in the presence of electron-electron interaction, similar to magnetic flux thus allowing backscattering processes, which involve tunneling through the puddle. Rectification of these fluctuations leads to a finite probability of backscattering. This effect is further enhanced due to dephasing process which is also dominated by zero-mode fluctuations. Remarkably, for temperature exceeding level spacing in the puddle, the rate of backscattering does not depend on temperature in a good agreement with recent experiments.

I. INTRODUCTION

Two-dimensional (2D) topological insulators (TI) — materials insulating in the bulk but having conducting helical edge states (HES) on the boundary — were predicted theoretically [1–3] and realized experimentally [4] more than fifteen years ago. The key property of the HES is spin-momentum locking, i.e. inversion of the spin direction with inversion of the electron momentum. This implies that HES form ideal ballistic conductors with topological protection against backscattering by non-magnetic disorder. However, experimentally this protection is effective only for short samples with length of HES not exceeding a few micron [5–7].

The backscattering can apparently appear due to scattering on magnetic impurities [8–10]. Conventional non-magnetic disorder can also lead to backscattering in TI edge in the presence of external magnetic field which breaks time reversal symmetry mixing opposite spin states [11]. The latter statement is supported by experiment, where a strong suppression of the edge conductance in external magnetic fields was demonstrated even in very short samples (with length of HES $\leq 1\mu\text{m}$), in particular, in 2D TI samples based on HgTe quantum wells (see [7] and references therein). However, the suppression of conductance is also clearly seen in the absence of external magnetic field for relatively long samples ($\geq 3\mu\text{m}$ for HgTe-based quantum well [7]). Importantly, the experimentally observed resistivity in this case is temperature-independent in a sufficiently wide range of temperatures (see inset in Fig. 1a of [7], where resistivity is independent of T within interval $1\text{ K} < T < 10\text{ K}$).

Several theoretical mechanisms were proposed to explain experimentally observed strong backscattering, in

particular, a mechanism involving magnetic impurities coupled to HES by exchange interaction [10, 12]. However, the presence of such impurities was never confirmed experimentally in structures where topological protection was broken in HES longer than a few microns (see discussion in Ref. [7]). Backscattering becomes possible in interacting systems: a mechanism assuming electron-electron scattering in HES in combination with conventional scattering was suggested in Ref. [13] as well as a mechanism involving spin-flip interaction-mediated scattering in a charge puddle tunnel-coupled to HES [14, 15]. Both mechanisms might, in principle, explain the observed violation of the topological protection. However, both scenarios predict strong increase of the backscattering conductance with temperature, particularly due to the temperature dependence of the phase volume available for inelastic scattering. Similarly, the point-like non-magnetic defects can also contribute to the backward scattering that essentially grows with temperature provided that interaction is taken into account [16]. Again, such strong temperature dependence of backscattering conductance is poorly supported by experimental data showing more or less constant backscattering rate within a wide temperature interval [7]. Backscattering in HES coupled to puddles were also predicted within semi-classical kinetic approach [17] that assumed phenomenologically introduced temperature-independent spin-flip collision rate [17] inside puddles, but physical mechanisms responsible for such spin-flip processes were not presented¹.

¹ Different regimes of e-e scattering in charge puddles were studied in [15]. It was shown there that the temperature independent backscattering conductance can be realized in conventional (non-topological puddles) interacting at very high temperatures higher than Δ/γ (for $\gamma \ll 1/g^{*2/3}$) or $g^* \sqrt{\gamma} \Delta$ (for $\gamma \gg 1/g^{*2/3}$), where Δ is the level spacing, γ is the tunneling transparency, and $g^* \gg$

* igor.krainov@mail.ru

In this Letter, we discuss HES tunnel-coupled to a puddle located near edge channel and suggest interaction-induced backscattering mechanism. In contrast to previously discussed mechanisms, our scenario does not involve inelastic scattering and therefore predicts temperature-independent backscattering rate in a wide temperature range. The underlying physics is based on the so-called zero-mode fluctuations in a puddle. We focus here on a simple model of a puddle—a cavity in the bulk of TI (see Fig. 1 a). Such cavities were already fabricated experimentally [18, 19]. They also have HES which are tunnel-coupled to the HES encompassing the TI; we will call these cavities topological puddles (TP). Another model of TP is a curved edge (see Fig. 1b) discussed previously for non-interacting case in Ref. [20] and curved edge with a spin-flip channels (see Fig. 1c) discussed in Ref. [21].

We analyze effect of the edge current in the TP. Although averaged value of this current is equal to zero, its zero-mode fluctuations act, in the presence of electron-electron interaction, similar to magnetic flux thus allowing backscattering processes, which involve tunneling through the puddle. Rectification of these fluctuations leads to a finite backscattering rate. This effect is further enhanced due to dephasing processes, in particular, by dephasing dominated by zero-mode fluctuations. Remarkably, for temperature exceeding level spacing in the puddle, the rate of backscattering does not depend on the amplitude of fluctuations (in contrast to previously discussed mechanisms of backscattering based on different models of puddles, where temperature-independent backscattering appeared at much higher T , see footnote ¹). This leads to temperature independent backscattering in the edge of topological insulator which may explain results of recent experiments, in particular, nearly constant edge resistivity observed in Ref. [7].

II. MODEL

A. Non-interacting case

The single-particle Hamiltonian of the TI is given by

$$H_0 = v_F \hat{p} \hat{\sigma}_z, \quad (1)$$

where $\hat{p} = -i\hbar\partial/\partial x$ is the electron momentum, $\hat{\sigma}_z$ is the Pauli matrix, and $-\infty < x < \infty$ is the coordinate along the edge of TI. The same Hamiltonian describes the edge of the TP with the replacement $x \rightarrow y$, where y is the coordinate along the edge of the TP which has a finite length L , so that $0 < y < L$ (see Fig. 1 b). For non-zero flux Φ through TP one should replace $-i\partial/\partial y \rightarrow -i\partial/\partial y + 2\pi\phi/L$, where $\phi = \Phi/\Phi_0$ and $\Phi_0 = hc/e$ is the

flux quantum. We model tunneling coupling between TI and TP by a point-like tunneling contact assuming that tunneling occurs between the point $x = 0$ of the TI edge and point $y = 0$ (or, equivalently, $y = L$) of the TP edge.

For non-interacting case, the edge conductance can be found with the use of the Landauer formula:

$$G = \frac{e^2}{h} \int dE |t(E)|^2 \left(-\frac{\partial f_F}{\partial E} \right), \quad (2)$$

where $t(E)$ is the transmission amplitude from $x = -\infty$ to $x = \infty$. with account of tunneling to TP and $f_F(E)$ is the Fermi distribution function.

Since transmission amplitude is evidently connected with the reflection amplitude $r(E)$ by the relation $|t(E)|^2 + |r(E)|^2 = 1$, the expression for conductance becomes:

$$G = \frac{e^2}{h} (1 - R_{bs}), \quad (3)$$

where $R_{bs} = \langle |r(E)|^2 \rangle_E$, where $\langle \dots \rangle$ stands for $\int dE (\dots) \partial f_F / \partial E$. In this Section we demonstrate that $r(E) \equiv 0$ for any E in the non-interacting case for zero magnetic field.

We describe the tunneling coupling between HES of TI and TP by the following scattering matrix [22]

$$\hat{S} = \begin{pmatrix} 0 & t & f & r \\ t & 0 & -r & f \\ -f & -r & 0 & t \\ r & -f & t & 0 \end{pmatrix}, \quad (4)$$

which connects outgoing and incoming amplitudes: $C'_i = S_{ij} C_j$, with $i, j = 1, \dots, 4$ (see Fig. 1a).

The phases of scattering amplitudes are irrelevant for the discussed problem, so we may choose t , r , and f to be real, so that

$$t^2 + r^2 + f^2 = 1.$$

The physical meaning of these amplitudes is illustrated in Fig. 1a. The amplitudes r and f describe hopping from HES states of TI to the HES of TP (and back to TI) with the same and opposite spin projections, respectively, while the amplitude t corresponds to propagation along HES (both in TI and in TP) without hopping (see also discussion in Ref. [21]). The corresponding rates can be parameterized as follows:

$$t^2 = 1 - 2\gamma, \quad r^2 = 2\gamma \cos^2 \beta, \quad f^2 = 2\gamma \sin^2 \beta, \quad (5)$$

The total probability of hopping between TI and TP is controlled by the tunneling transparency γ ($0 < \gamma < 1/2$). For tunneling contact, this parameter is small, $\gamma \ll 1$, and is largely controlled by the tunneling distance. The case of “metallic” contact, when TI and TP are strongly coupled, can be modeled by $\gamma \approx 1/2$. The parameter β controls spin-flip processes, so that for $\beta = 0$ we have $f = 0$. Different geometries of the edge and cavity are shown in Fig. 1 (see also discussion below in Sec. V).

¹ is the dimensionless conductance of the diffusive puddle. Such temperatures are much higher than Δ .

Already at the level of Eq. (4) and Fig. 1 one can notice the appearance of certain processes of backscattering in the HES of TI for $f \neq 0$. To demonstrate it, we calculate the reflection amplitudes describing two different scattering processes $1 \rightarrow 1'$ in Fig. 1.

Let us consider propagation of the particle with wave-vector k and energy $E = \hbar v_F k$ from $x = -\infty$. The total backscattering amplitude consists of two contributions,

$$r(E) = r_R + r_L,$$

corresponding to clockwise, $r_R = r_R(E)$, and counterclockwise propagation, $r_L = r_L(E)$, around the edge of the puddle.

The amplitude r_R describes hopping from 1 to 3' with amplitude f , rotation clockwise with arbitrary number of winding and hopping back from 4 to 1' with amplitude r . Each winding around the edge of the island yields factor te^{ikL} . Summing over winding number n , we arrive at:

$$r_R = fe^{ikL} \sum_{n=0}^{\infty} (te^{ikL})^n r = \frac{fre^{ikL}}{1 - te^{ikL}}.$$

Amplitude r_L describes hopping from 1 to 4' with amplitude r , rotation counterclockwise with arbitrary number of winding and hopping back from 3 to 1' with amplitude $-f$. Summing over winding number, we get:

$$r_L = re^{ikL} \sum_{n=0}^{\infty} (te^{ikL})^n (-f) = -\frac{fre^{ikL}}{1 - te^{ikL}}.$$

We see that both contributions depend on the electron energy through the wave vector k . Each of these contributions taken separately would lead to backscattering. However, as we see from above equations, the total backscattering amplitude is zero for any energy:

$$r(E) = r_R + r_L \equiv 0,$$

so that the single particle picture, as expected, do not lead to backscattering due to time-reversal symmetry.

In the presence of external magnetic field, phases additional to kL appear, which have opposite signs for opposite chiralities: $\varphi_R = kL - 2\pi\phi$, $\varphi_L = kL + 2\pi\phi$. The resulting amplitudes r_R and r_L no longer cancel each other and $r(E) \neq 0$.

B. Interacting case

Remarkably, the total backscattering amplitude is also non-zero in the interacting case due to the so-called zero-mode (ZM) fluctuations. Next, we discuss the underlying physics of ZM fluctuations which were previously studied in context of tunneling transport through Aharonov-Bohm interferometer made of conventional single-channel wire in spinless [23, 24] and spinful [25] cases. We will take into account interaction within HES of TP, for

$0 < y < L$, assuming that the dimensionless interaction constant, g , is small, $g \ll 1$ ². We do not take into account interaction between states of the same chirality, since it only leads to renormalization of the Fermi velocity.

Interaction of the electrons with the opposite chiralities is described by the following Hamiltonian

$$\hat{H}_{\text{int}} = 2\pi\hbar v_F g \int_0^L dy \hat{n}_R \hat{n}_L, \quad (6)$$

where $\hat{n}_{R,L}(y)$ are densities of the right- and left-moving electrons. This interaction leads to propagation of fermionic excitations with plasmonic velocity $u = v_F \sqrt{1 - g^2}$ [26].

In the secondary quantization representation, the non-interacting Hamiltonian of the system can be expressed in terms of field operators describing the electrons in two terminals μ_a and μ_b connected with the helical edge of TI (see Supplementary material):

$$H_0 = \sum_k \hbar v_F k \left(\hat{c}_k^{\dagger} \hat{c}_k^a + \hat{c}_k^{\dagger} \hat{c}_k^b \right) \quad (7)$$

where $\hat{c}_k^{a(b)}$ are the electron annihilation operators in the reservoir $\mu_{a(b)}$. The interaction term Eq. (6) can be also expressed in terms of $\hat{c}_k^{a(b)}$ with the use of Eqs. (A5), (A6), and (A11) of the Supplementary material.

Rigorous calculation of conductance can be performed with the use of the Kubo formula. This calculation is quite tricky and will be presented elsewhere [27].

Here, we demonstrate that our key result — strong backscattering induced by interaction can be obtained by using the quasiclassical approximation based on several assumptions. First of all, we assume that typical wave vector of inhomogeneity of the problem is small compared to the Fermi wave vector

$$q \sim 1/L \ll k_F.$$

Secondly, we assume that the electron-electron interaction is weak: $g \ll 1$ and $g^2 \Lambda \ll 1$, where $\Lambda = \ln(E_F/T) \gg 1$ and E_F is the Fermi energy ($E_F \gg T$). These conditions allow one to neglect renormalization corrections specific for the Luttinger liquid [26]. Such corrections will be briefly discussed separately in the end of the paper in Sec. V. Importantly, they only lead to renormalization of the scattering matrix and do not change physics of the effect under discussion. We will also assume that

$$T \gg \Delta, \quad (8)$$

² Following Luttinger liquid notations [26], we assume the interaction of the form, $\frac{1}{2}g_4(n_R(x)^2 + n_L(x)^2) + g_2 n_R(x)n_L(x)$, and set $g_4 = 0$, $g_2 = 2\pi v_F g$ afterwards.

where

$$\Delta = \frac{2\pi u}{L} \approx \frac{2\pi v_F}{L} \quad (9)$$

is the level spacing in the edge of TP. Typical value of Δ for a TP with L about $1 \mu\text{m}$ is 1 K . Hence, inequality (8) is satisfied in experiment [7] as seen from inset in Fig. 1a of this work, where experimentally measured value of the resistivity was approximately constant within the temperature interval $1 \text{ K} < T < 10 \text{ K}$.

The effect of electron-electron interaction on the single-particle transmission amplitudes is described within this approximation in terms of scattering on the thermal electromagnetic noise created by the bath of other electrons. We will see that the key parameter describing interaction within such an approach is $g\sqrt{T/\Delta} \gg g$.

Within quasiclassical approximation, we replace in the exact quantum equations for field operators in the Heisenberg approximation (see Eq. (A12) in the Supplementary material) the quantum density operators \hat{n}_R and n_L with the quasiclassical densities, which depend on y and t through the combinations $y - ut$ and $y + ut$, respectively. Since interaction term is proportional to g , one can replace $u \approx v_F$, thus arriving to the following equations inside the TP edge

$$\begin{aligned} i \left(\frac{\partial}{\partial t} + v_F \frac{\partial}{\partial y} \right) \hat{\Psi}_R &= 2\pi v_F g n_L(y + v_F t) \hat{\Psi}_R, \\ i \left(\frac{\partial}{\partial t} - v_F \frac{\partial}{\partial y} \right) \hat{\Psi}_L &= 2\pi v_F g n_R(y - v_F t) \hat{\Psi}_L, \end{aligned} \quad (10)$$

where field operators $\Psi_{R,L}$ are defined in the Supplementary material. These equations coincide with the ones describing motion in the electron in the dynamical potential

$$\begin{aligned} \hat{U}(y, t) &= \sum_n \begin{pmatrix} U_{L,n} e^{iq_n(y-v_F t)} & 0 \\ 0 & U_{R,n} e^{iq_n(y+v_F t)} \end{pmatrix}, \\ U_{R,n} &= 2\pi \hbar g v_F \int_0^L n_L(y) e^{-iq_n y} dy / L, \\ U_{L,n} &= 2\pi \hbar g v_F \int_0^L n_R(y) e^{-iq_n y} dy / L, \end{aligned} \quad (11)$$

where $q_n = 2\pi n/L$.

The Hamiltonian $\hat{H}_0 + \hat{U}$ with \hat{H}_0 given by Eq. (1) consists of the quasistatic part $\hat{H}_0 + \hat{U}_0$, where \hat{U}_0 is the part of \hat{U} with $n = 0$, and rapidly oscillating dynamical part described by \hat{U}_n with $n \neq 0$. As we demonstrate in the Supplementary material, the rapidly oscillating terms can be treated perturbatively and do not lead to any transitions within standard golden-rule calculation. Hence, we neglect these terms.

The quasistatic matrix potential reads

$$\hat{U} = \begin{pmatrix} U_{L,0} & 0 \\ 0 & U_{R,0} \end{pmatrix}, \quad (12)$$

where $U_{L,0} = 2\pi \hbar v_F g N_R/L$, $U_{R,0} = 2\pi \hbar v_F g N_L/L$, and

$$N_{R,L} = \int_0^L dy n_{R,L}$$

are the total numbers of the right- and left-moving electrons in the edge of TP. The Hamiltonian (12) exists in the edge of TP.

Numbers $N_{R,L}$ are integer and can slowly fluctuate due to tunneling coupling with the edge of TI. As a first step, we neglect slow dynamics of $N_{R,L}$ assuming that these are static integer numbers. Then, we arrive at single-particle static problem described by the Hamiltonian $H_0 + \hat{U}_0$ and scattering matrix Eq. (4). This problem can be easily solved exactly. The scattering waves for this Hamiltonian are presented in the Supplementary material [see Eq. (C1)]. Most importantly, in this solution, backscattering amplitude is non-zero:

$$r_{bs} = rf \left[\frac{e^{i\varphi_R}}{1 - t e^{i\varphi_R}} - \frac{e^{i\varphi_L}}{1 - t e^{i\varphi_L}} \right], \quad (13)$$

where

$$\begin{aligned} \varphi_R &\approx kL - 2\pi\phi + 2\pi g N_L, \\ \varphi_L &\approx kL + 2\pi\phi + 2\pi g N_R. \end{aligned} \quad (14)$$

Here $2\pi g N_{R,L}$ are interaction-induced corrections to the phases acquired by the electrons with opposite chiralities after propagation around the edge TP (similar result was obtained in Refs. [23, 24] for conventional interferometer). These phase corrections lead to dependence of r_{bc} on $N_{R,L}$ and we also need to perform average on distribution and dynamics of these numbers, which may fluctuate due to tunneling coupling of the TP with HES of TI. However, for small γ , this dynamics is slow and in the first approximation, one can assume that these numbers are ‘‘frozen’’ and distributed according to the Gibbs distribution. The next step is to consider dynamics of these fluctuations similarly to Refs. [23–25]. We perform the corresponding calculations below.

III. STATIC FLUCTUATIONS

We start our analysis by considering static fluctuations in TP and regard backscattering of a single electron on the thermal bath of remaining electrons characterized by certain fixed values of $N_{R,L}$.

The reflection amplitude in HES is given for fixed $N_{R,L}$ by Eq. (13) with phases $\varphi_{R,L}$ given by Eq. (14). The external magnetic field and the electron-electron interaction induce the phase difference:

$$\delta\varphi = \varphi_R - \varphi_L = -4\pi\phi - 2\pi g J, \quad (15)$$

where

$$J = N_R - N_L, \quad (16)$$

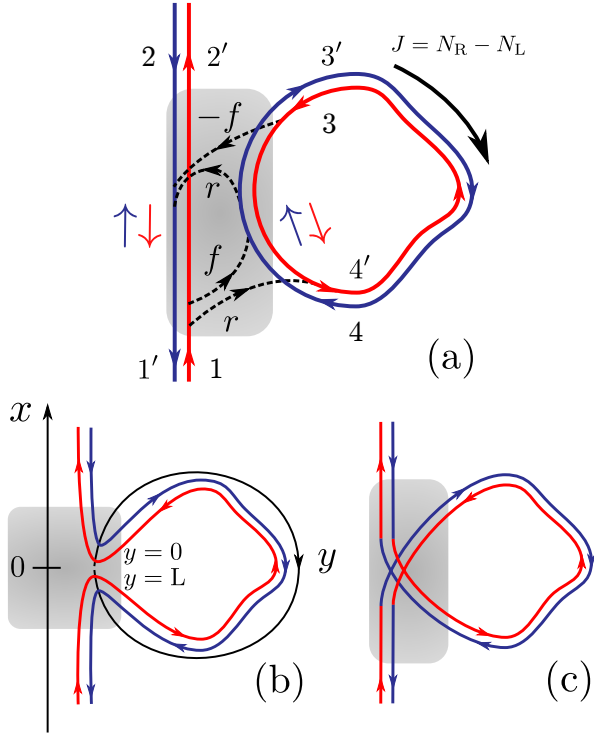


FIG. 1. (a) Topological puddle, formed by a cavity in the bulk of TI, tunnel-coupled to the HES of TI. Contact region is shown by gray color. Dashed lines illustrate two processes corresponding to backscattering $1 \rightarrow 1'$: (i) jump from 1 to $3'$ with amplitude f , rotation clockwise with arbitrary number of winding and jump back to $1'$ with amplitude r ; (ii) jump from 1 to $4'$ with amplitude r , rotation counterclockwise with arbitrary number of winding and jump back to $1'$ with the amplitude $-f$; (b) and (c) different geometries of the contact described by the same \hat{S} matrix (see Eq. (4)): (b) curved edge [20], (c) contact with spin-flip channels [21].

is the persistent current circulating along the edge of the TP. Importantly, $\delta\varphi$ does not depend on k and, consequently, on the energy of the tunneling electron. The backscattering probability for fixed $N_{R,L}$ is given by

$$R_{bs} = |r_{bs}|^2 = \frac{4r^2 f^2 \sin^2(\delta\varphi/2)}{|1 - t e^{i\varphi_R}|^2 |1 - t e^{i\varphi_L}|^2}. \quad (17)$$

This equation still depends on k , entering the phases $\varphi_{R,L}$.

Next, we average over the electron energy assuming that the inequality Eq. (8) is satisfied. Importantly, Fermi distribution function change on the energy scale on the order of T scale, while the reflection amplitude $r(E)$ oscillates on the much smaller scale Δ . Hence, one can first average over fast oscillation on the Δ scale neglecting variation of the distribution function and next average thus obtained equations over the temperature window. To this end, we replace in Eq. (17) $e^{ikL} \rightarrow z$ and integrate over complex variable z along the contour $|z| = 1$, having in mind that $t < 1$. The integral is given by contributions of two poles located inside this contour.

The result of such calculation depends on parameters of S -matrix and phase $\delta\varphi$:

$$\begin{aligned} \langle R_{bs} \rangle_E &= \frac{4r^2 f^2}{r^2 + f^2} \frac{(1 + t^2) \sin^2(\delta\varphi/2)}{(r^2 + f^2)^2 + 4t^2 \sin^2(\delta\varphi/2)} \\ &= \frac{\gamma(1 - \gamma) \sin^2(2\beta) \sin^2(\delta\varphi/2)}{\gamma^2 + (1 - 2\gamma) \sin^2(\delta\varphi/2)}. \end{aligned} \quad (18)$$

Equation similar to Eq. (18) was obtained previously in Ref. [20] for non-interacting ($g = 0$) ensemble of TP having different dynamical phases kL , zero temperature and non-zero magnetic field.

In the absence of magnetic field, $\delta\varphi$ is solely determined by the persistent current in the TP,

$$\delta\varphi = -2\pi gJ. \quad (19)$$

In the limit $g \rightarrow 0$, Eq. (18) takes on a perturbative form with respect to the interaction

$$\langle R_{bs} \rangle_E = \frac{4\pi^2 g^2 r^2 f^2 (1 + t^2) J^2}{(1 - t^2)^2}. \quad (20)$$

Replacing in this formula $J^2 \rightarrow J_{rms}^2$ (see Eq. (27) below) one gets perturbative result, which can be obtained by direct summation of relevant diagrams up to the second order with respect to g [27]. On the other hand, as seen from Eq. (18), perturbation theory fails already at sufficiently weak interaction. Indeed, assuming weak tunneling coupling, $\gamma \ll 1$ we arrive at the following expression

$$\langle R_{bs} \rangle_E = \frac{\gamma \sin^2(2\beta) \sin^2(\pi gJ)}{\gamma^2 + \sin^2(\pi gJ)}. \quad (21)$$

Since γ is small, the term $\sin^2(\pi gJ)$ in the denominator becomes relevant at not too large g . Let us discuss this issue in more detail. Equation (18) with $\delta\varphi$ given by Eq. (19) gives probability of backscattering at fixed $N_{R,L}$ averaged over E within the temperature window. As we mentioned above, $N_{R,L}$ and, consequently, J fluctuate. The energy of these fluctuations, the so-called zero mode energy, was first derived in the theory of the Luttinger liquid [28, 29]:

$$\begin{aligned} \epsilon_{N_L, N_R} &= \frac{\Delta}{4K} [(N_L + N_R - 2N_0)^2 \\ &\quad + K^2(N_L - N_R - 2\phi)^2], \end{aligned} \quad (22)$$

where $K = \sqrt{(1 - g)/(1 + g)} \approx 1 - g$ is the so-called Luttinger parameter and N_0 is averaged value of $N_{R,L}$. The probability of fluctuation with given numbers N_R and N_L is given by the Gibbs weight

$$f_{N_L, N_R} = Z^{-1} e^{-\epsilon_{N_R, N_L}/T}, \quad (23)$$

where $Z = \sum_{N_R, N_L} e^{-\epsilon_{N_R, N_L}/T}$.

Next step is to average Eq. (21) over zero-mode fluctuations. Since by assumption, $g \ll 1$, one can neglect g

in the expression for zero mode energy. [Accounting of g in ZM energy leads to small corrections on the order of $g \ll 1$, while we focus on corrections $\propto gJ$, which are much larger, since fluctuations of J are large, $J \gg 1$ (see Eq. (27) below).] Due to the same reason, one can also neglect ϕ in ϵ_{N_R, N_L} . Then, expression for the zero-mode energy simplifies

$$\epsilon_{N_R, N_L} \approx \frac{\Delta}{2} [(N_R - N_0)^2 + (N_L - N_0)^2]. \quad (24)$$

This equation can be easily derived without using formalism of the Luttinger liquid. To this end, we assume that TP is weakly coupled with the edge of TI and therefore, in the first approximation, the puddle is closed. Then, one can introduce quantum levels in the edge of TP numerated by index j with the energy $E_j = \Delta j$ and population $n_{R,j}$ and $n_{L,j}$ which can be 1 with the probability $f_j = f_F(E_j)$ and 0 with the probability $1 - f_j$. Then, expressing $N_{R,L}$ in terms of $n_{R,j}, n_{L,j}$,

$$N_R = \sum_j n_{R,j}, \quad N_L = \sum_j n_{L,j}, \quad (25)$$

and writing distribution function as $f_{N_R, N_L} = \langle \delta_{N_R, \sum_j n_{R,j}} \delta_{N_L, \sum_j n_{L,j}} \rangle$ (here $\delta_{N, N'}$ is the Kronecker index and averaging is taken over realizations of $n_{R,j}, n_{L,j}$), and using identity, $\delta_{N, N'} = \int_0^{2\pi} \exp[i\chi(N - N')] d\chi / 2\pi$, we get

$$\begin{aligned} f_{N_R, N_L} &= \int \frac{d\chi_R}{2\pi} \frac{d\chi_L}{2\pi} \left\langle e^{i\chi_R(\sum_j n_{R,j} - N_R) + i\chi_L(\sum_j n_{L,j} - N_L)} \right\rangle \\ &= \int \frac{d\chi_R}{2\pi} \frac{d\chi_L}{2\pi} e^{-i(\chi_R N_R + \chi_L N_L)} \\ &\quad \times \prod_j [(1 - f_j + f_j e^{i\chi_R}) (1 - f_j + f_j e^{i\chi_L})]. \end{aligned} \quad (26)$$

Using expansion $\ln[1 - f_j + f_j e^{i\chi}] \approx if_j \chi - f_j(1 - f_j)\chi^2/2$ valid for small χ and then integrating over $\chi_{R,L}$ with the use of properties $N_0 = \sum_j f_j$, $\sum_j f_j(1 - f_j) \approx T/\Delta$, we

restore Eq. (23) with ϵ_{N_R, N_L} given by Eq. (24). A more rigorous derivation of ZM distribution function assuming Fermi-Dirac distribution in the leads connected to the system is based on the spectral determinants approach. We delegate corresponding calculation to the Supplementary material.

Now, we are in position to average over static zero-mode fluctuations. The average value of the current with zero-mode distribution function is zero, but its root mean square (rms) value is non-zero and sufficiently large:

$$J_{\text{rms}} = \sqrt{\langle J^2 \rangle_{\text{ZM}}} = \sqrt{\sum_{N_R, N_L} J^2 f_{N_R, N_L}} \approx \sqrt{2T/\Delta} \gg 1, \quad (27)$$

where $\langle \dots \rangle_{\text{ZM}}$ stands for the zero-mode averaging with function (23). The current J in Eq. (15) acts similar to

the fluctuating magnetic flux. Hence, underlying physics of backscattering mechanism is rectification of fluctuations of this effective “magnetic flux”. It is worth stressing that this mechanism does not involve inelastic scattering and dephasing and only uses thermodynamical averaging over static zero-mode current fluctuations. In the next section we demonstrate that dephasing processes suppress destructive interference between right- and left-propagating waves and, consequently, additionally enhance backscattering.

Assuming $\gamma \ll 1$, and $\gamma \ll g\sqrt{T/\Delta}$ we obtain after averaging Eq. (21) with statistical weight (23):

$$\mathcal{R} = \langle R_{\text{bc}} \rangle_{E, \text{ZM}} = \sum_{N_R, N_L} f_{N_R, N_L} \langle R_{\text{bc}} \rangle_E \approx \gamma \sin^2(2\beta). \quad (28)$$

Hence, we get temperature-independent scattering rate.

The above condition $\gamma \ll g\sqrt{T/\Delta}$ deserves a special comment. Rewriting it as $T \gg \Delta\gamma^2/g^2$, we see that it is much stronger than the inequality (8) for $\gamma \gg g$. However, we will demonstrate below that the consideration of zero mode dynamics leads to softening of this condition, so that the inequality (8) is the only limitation required for T ³.

IV. EFFECT OF DEPHASING

We assumed above that the numbers $N_{R,L}$ are fixed, so that the “electron bath”, created by the electrons propagating in the edge of TP, is frozen. Such approximation implies that dephasing processes are absent. In this section we demonstrate that dephasing increases backscattering. We start with discussion of general dephasing mechanism with the dephasing rate Γ_φ and then consider dephasing caused by dynamics of zero-mode fluctuations.

A. General dephasing mechanism

We start with separating in the energy-averaged backscattering rate classical and interference contributions:

$$\mathcal{R} = \mathcal{R}^{\text{cl}} + \mathcal{R}^{\text{int}} \quad (29)$$

Here,

$$\begin{aligned} \mathcal{R}^{\text{cl}} &= r^2 f^2 \left\langle \left| \frac{1}{1 - te^{i\varphi_R}} \right|^2 + \left| \frac{1}{1 - te^{i\varphi_L}} \right|^2 \right\rangle_{E, \text{ZM}} \\ &= \frac{2r^2 f^2}{1 - t^2} \end{aligned} \quad (30)$$

³ The factor $\sin^2(2\beta)$ also deserves a comment. Backscattering appears only for $\beta \neq 0$, so that the spin-quantization axes in the HES of TI and TP should be different. This implies spin-orbit interaction in the contacts which is responsible for momentum needed for an electron to backscatter

is the classical contribution given by sum of squared amplitudes of right- and left-propagating waves [see Eq. (13)]. This contribution is insensitive to zero-mode fluctuations and dephasing. The contribution describing interference between right- and left-propagating waves reads

$$\begin{aligned}\mathcal{R}^{\text{int}} &= -r^2 f^2 \left\langle \frac{e^{i(\varphi_R - \varphi_L)}}{(1 - te^{i\varphi_R})(1 - te^{-i\varphi_L})} + \text{h.c.} \right\rangle_{E, \text{ZM}} \\ &= -r^2 f^2 \sum_{n=1}^{\infty} t^{2(n-1)} \langle e^{i\delta\phi n} \rangle_{\text{ZM}} + \text{h.c.},\end{aligned}\quad (31)$$

where $\delta\phi$ is given by Eq. (15). Bottom line of this equation is obtained by expanding

$$\frac{1}{(1 - te^{i\varphi_R})(1 - te^{-i\varphi_L})} = \sum_{n=1}^{\infty} \sum_{m=1}^{\infty} t^{n+m} e^{in\varphi_R - im\varphi_L}$$

and noticing that terms with $m \neq n$ drop out after the energy averaging: $\langle \exp[ikL(n-m)] \rangle_E = 0$.

Summing in Eq. (31) goes over winding number n . Since n windings takes nL/v_F time, we can introduce phase breaking time by inserting a factor $\exp[-\Gamma_\varphi nL/v_F]$ in the argument of sum in Eq. (31). Then, expression for \mathcal{R} becomes

$$\begin{aligned}\mathcal{R} &= r^2 f^2 \sum_{N_R, N_L} f_{N_R, N_L} \left[\frac{2}{1 - t^2} - \left(\frac{1}{1 - t^2 + z} + \text{h.c.} \right) \right] \\ &= \gamma^2 \sin^2(2\beta) \sum_{N_L, N_R} f_{N_R, N_L} \left[\frac{1}{\gamma} - \frac{2(2\gamma + z_1)}{(2\gamma + z_1)^2 + z_2^2} \right],\end{aligned}\quad (32)$$

where z_1 and z_2 are real and imaginary parts of $z = e^{\Gamma_\varphi L/v_F - i\delta\phi} - 1$. Introducing dimensionless dephasing rate,

$$\gamma_\varphi = \frac{\pi\Gamma_\varphi}{\Delta},$$

and assuming that dephasing is not too fast, $\gamma_\varphi \ll 1$, we find that for small $\delta\phi$, such that $\delta\phi \lesssim \gamma + \gamma_\varphi \ll 1$ Eq. (32) simplifies

$$\begin{aligned}\mathcal{R} &= \gamma^2 \sin^2(2\beta) \\ &\times \sum_{N_L, N_R} f_{N_L, N_R} \left[\frac{1}{\gamma} - \frac{\gamma_\varphi + \gamma}{(\gamma_\varphi + \gamma)^2 + (\pi gJ + 2\pi\phi)^2} \right].\end{aligned}\quad (33)$$

First and second terms in the square brackets represent, respectively, classical and interference contributions, which cancel each other when γ_φ, ϕ , and J equal to zero.

Equations (32) and (33) represent the central result of our work. As seen, for zero magnetic field ($\phi = 0$) both dephasing and current fluctuations suppress interference term thus destroying destructive interference and leading to universal expression Eq. (28), which does not depend on temperature and properties of TP, and is fully

expressed via matrix elements of the scattering matrix. This is the same result as for static fluctuations but the condition on temperature is weaker, $T \gg \Delta$, provided that $\gamma_\varphi \gg \gamma$. The physics behind the softening of the condition on the temperature is clarified by considering the second line in Eq. (33). The interference term depends both on J and γ_φ . In the absence of dephasing (and for $\phi = 0$), non-zero \mathcal{R} appears only for $J \neq 0$. By contrast, for $\gamma_\varphi \gg \gamma$, the second term is small for any value of J . In other words, fast dephasing suppress interference term and, hence, destroys compensation of the classical and quantum contributions. Most importantly, for intensive dephasing, $\gamma_\varphi \gg \gamma$, Eq. (28) is valid independently on the strength of the tunneling coupling and electron-electron interaction.

B. Dephasing due to dynamics of zero-mode fluctuations

We assumed above that the numbers $N_{R,L}$ are fixed, so that the “electron bath” of the electrons propagating in the edge of TP is frozen, i.e. numbers $n_{R,j}, n_{L,j}$ and, consequently, $N_{R,L}$ are fixed, while dephasing is governed by external fluctuating bath. Actually, the numbers $N_{R,L}$ slowly change in time on the scale $\propto 1/\gamma\Delta$ due to tunneling coupling with the edge of TI,

$$N_R(t) = \sum_j n_{R,j}(t), \quad N_L = \sum_j n_{L,j}(t), \quad (34)$$

thus also resulting in dephasing which suppresses the interference term \mathcal{R}^{int} . In order to calculate corresponding dephasing rate we first rewrite ZM average in the bottom line in Eq. (31) with the use of Eq. (26) as follows (here, we put $\phi = 0$)

$$\begin{aligned}\langle e^{in\delta\phi} \rangle_{\text{ZM}} &= \sum_{N_R, N_L} f_{N_R, N_L} e^{-igJ(N_R - N_L)\Delta t_n} \\ &= \prod_j \langle e^{ign_{R,j}\Delta t_n} \rangle \langle e^{-ign_{L,j}\Delta t_n} \rangle,\end{aligned}\quad (35)$$

where $t_n = nL/v_F$ and averages

$$\langle e^{ign_{R,j}\Delta t_n} \rangle = \langle e^{-ign_{L,j}\Delta t_n} \rangle^* = (1 - f_j + f_j e^{ig\Delta t_n}) \quad (36)$$

are taken over realizations of level population numbers: $n = 1$ with probability f and $n = 0$ with probability $(1 - f)$. Here and in what follows, for simplicity, we skip indexes R, L, j at $n_{R,j}$ and $n_{L,j}$, and also index j at f_j .

Since $n(t)$ changes very slowly, one can take into account the ZM dynamics by replacing $\langle e^{ign\Delta t_n} \rangle \rightarrow \langle e^{ig \int_0^{t_n} dt n(t)\Delta} \rangle$. Hence, the problem reduces to dynamics of single level population.

The occupation number fluctuates between two values, 0 and 1. Hence, the time evolution of these numbers is a telegraph noise with the rates Γf_j and $\Gamma(1 - f_j)$ for scattering “in” (population rate of an empty level with

$n_j = 0$) and “out” (depopulation rate of an occupied level with $n_j = 1$), respectively. Here, Γ is the tunneling rate, which is connected with the tunneling transparency as follows

$$\Gamma = \frac{\gamma\Delta}{\pi}, \quad (37)$$

and we take into account that equilibrium distribution function f_j at the energy of the j th level is the same for the same energy of the TI edge.

The phase factor induced by the interaction with a certain quantum level is written as [23, 24] (a similar approach was used to describe dephasing of a qubit by a two level fluctuator, see Refs. [30–32] and references therein):

$$\begin{aligned} \left\langle \exp \left(ig\Delta \int_0^t d\tau n(\tau) \right) \right\rangle &= \\ &= (1-f)(P_{00} + P_{01}) + f(P_{10} + P_{11}), \end{aligned} \quad (38)$$

where $P_{\alpha\beta}$ ($\alpha, \beta = 0, 1$) is an expectation value for the phase factor $\exp \left(ig\Delta \int_0^t d\tau n(\tau) \right)$ with fixed initial and final occupation of the level given by α and β , respectively. For example, P_{01} describes process, where level was empty ($n = 0$) for $t = 0$ and occupied ($n = 1$) at the moment t . Functions $P_{\alpha\beta}$ obey master equations

$$\begin{aligned} \frac{dP_{00}}{dt} &= -\Gamma f P_{00} + \Gamma(1-f)P_{01}, \\ \frac{dP_{10}}{dt} &= -\Gamma f P_{10} + \Gamma(1-f)P_{11}, \\ \frac{dP_{01}}{dt} &= [-\Gamma(1-f) + 2i\pi g\Delta] P_{01} + \Gamma f P_{00}, \\ \frac{dP_{11}}{dt} &= [-\Gamma(1-f) + 2i\pi g\Delta] P_{11} + \Gamma f P_{10}, \end{aligned} \quad (39)$$

which should be solved with the following initial conditions $P_{01}(0) = P_{10}(0) = 0$, $P_{00}(0) = P_{11}(0) = 1$. Solving Eq. (39) and substituting the result into Eq. (35) we get (see discussion in Refs. [23, 24])

$$\langle e^{in\delta\varphi} \rangle_{\text{ZM}} \approx \exp \left[-\frac{2T}{\Delta} (1 - \cos(g\Delta t)) \right] e^{-\Gamma_\varphi t}, \quad (40)$$

where first exponent describes static fluctuations

$$\sum_{N_R, N_L} f_{N_R, N_L} e^{-igJ\Delta t} \approx \exp \left[-\frac{2T}{\Delta} (1 - \cos(g\Delta t)) \right], \quad (41)$$

while the second one is responsible for dephasing with the following rate $\Gamma_\varphi = 4\Gamma T/\Delta$. Corresponding dimensionless dephasing is given by

$$\gamma_\varphi = 4\gamma T/\Delta. \quad (42)$$

Hence, dephasing rate due to the telegraph noise is much higher than tunneling rate, so that $\gamma_\varphi \gg \gamma$, interference term, \mathcal{R}^{int} , is suppressed and backscattering rate is given by Eq. (28)

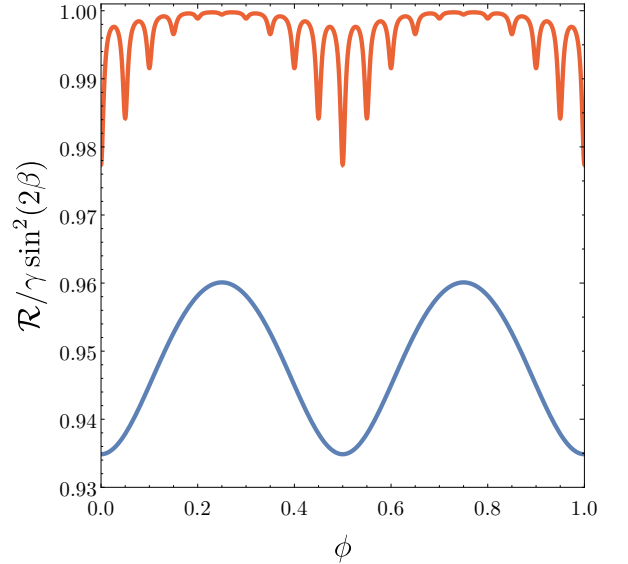


FIG. 2. Dependence of backscattering probability on magnetic flux calculated by using second line of Eq. (33) for $T/\Delta = 3$, $g = 0.1$, γ_φ given by Eq. (42), and different tunneling couplings: $\gamma = 0.003$ (red curve) and $\gamma = 0.07$ (blue curve).

Due to intensive dephasing, the interference contribution is small but depends on magnetic flux demonstrating Aharonov-Bohm oscillations with the amplitude smaller than the classical contribution by a factor $\sim \gamma/\gamma_\varphi \sim \Delta/T$. These oscillations are shown in Fig. 2. Similar to conventional interferometers [23], the shape of the oscillations depends on the relation between γ_φ and g : sharp peaks separated by distance $\delta\phi = g/2$ for $\gamma_\varphi \ll g$ (red curve in Fig. 2) and harmonic oscillations with the period $\delta\phi = 1/2$ for $\gamma_\varphi \gg g$ (blue curve in Fig. 2).

V. RENORMALIZATION OF SCATTERING MATRIX

We see that backscattering probability within a model with temperature-independent parameters of S -matrix does not depend on temperature. Actually, slow dependence on temperature arises due to interaction-induced renormalization of γ and β [22, 33]. Corresponding renormalization group (RG) equations look

$$\begin{aligned} \frac{d\gamma}{d\Lambda} &= -g^2\gamma(1-2\gamma)(1-4\gamma+\gamma\sin^2(2\beta)), \\ \frac{d\beta}{d\Lambda} &= -\frac{1}{4}g^2\gamma\sin(4\beta). \end{aligned} \quad (43)$$

Here $\Lambda = \log E_F/E$. These equations describe flow of γ and β in the interval between $E = E_F$ and $E = T$. They have a stable fixed line $\gamma = 0$ (L1) and two fixed stable points: FP2 ($\gamma = 1/2, \beta = 0$) and FP3 ($\gamma = 1/2, \beta = \pi/2$). Three different stable phases corresponding to L1,

FP2, and FP3 are separated by three lines intersecting in the fully unstable multicritical point (see full diagram of RG flow in Ref. [21]). The vicinity of L1, FP2, and FP3, roughly speaking, correspond to the geometries shown in Fig. 1 in the panels (a), (b), and (c), respectively.

Importantly, the RG flow predicted by Eq. (43) is very slow since the right hand side of these equations is proportional to g^2 . Particularly, in case of the weak tunneling coupling, $\gamma \ll 1$, depicted in Fig. 1a, the backscattering probability determined by the last line in Eq. (33) obeys

$$\frac{d\mathcal{R}}{d\Lambda} = -g^2\mathcal{R}. \quad (44)$$

The solution of this equation shows that the tunneling coupling and, consequently, the backscattering probability slowly depends on temperature

$$\mathcal{R} = \mathcal{R}_0 \left(\frac{T}{E_F} \right)^{g^2}, \quad (45)$$

where \mathcal{R}_0 is the “bare” value observed at high temperatures, $T \sim E_F$.

Both stable fixed points FP2 and FP3 correspond to “metallic” contact, $\gamma \rightarrow 1/2$. For such a contact, the main contribution to \mathcal{R} comes from trajectories with a single winding. By using Eq. (18), we find in vicinity of FP2 and FP3: $\mathcal{R} \approx 4(\delta\beta)^2 \langle \sin^2(\delta\varphi/2) \rangle_{\text{ZM}} \approx 2(\delta\beta)^2$ for high T . Here $\delta\beta = \beta \ll 1$ for FP2 and $\delta\beta = \pi/2 - \beta \ll 1$ for FP3. As follows from RG equations, $(\delta\beta)^2$ scales with the same critical index g^2 , so that Eqs. (44) and (45) equally apply at sufficiently high temperature in the vicinity of L1, FP2 and FP3.

VI. CONCLUSION

In this Letter, we investigated backscattering mechanism for helical edge states in two-dimensional topological insulator which is coupled—by tunneling or quasimetallic contact—to an interacting puddle located near the edge channel. Such a puddle can be created artificially by making a cavity in the bulk of a topological insulator, tunnel-connected to the edge states (see Fig. 1a). Also, a puddle can appear when the boundary of the sample is strongly curved (see Fig. 1b,c). The suggested mechanism is based on the interaction-induced phase difference between the electron waves propagating around the edge of the puddle clockwise and counterclockwise. This phase difference allows for backscattering inside the edge of the topological insulator in the processes involving tunneling through the puddle. It is proportional to the fluctuating edge current, J , that circulates around the puddle. Statistics and dynamics of J are fully determined by the zero-mode fluctuations. The backscattering probability is nonlinear function of J , so that the rectification of the fluctuations leads to non-zero backscattering rate, which is further increased by zero-mode dephasing. Importantly, suggested mechanism does not involve

inelastic scattering and is temperature-independent (up to a slow scaling due to renormalization of the tunneling amplitudes) at sufficiently high temperatures. For weak tunneling coupling, the backscattering rate saturates at temperature-independent level proportional to the tunneling transparency,

$$\mathcal{R} \propto \gamma, \quad (46)$$

provided that temperature exceeds the level spacing in the puddle: $T \gg \Delta$.

We considered here simplest model of a ballistic topological puddle. Simple estimates show that similar temperature-independent (or showing very weak logarithmical temperature dependence) backscattering should occur in the diffusive island tunnel-coupled to the edge of TI [27]. Such temperature-independent suppression of conductance is in good agreement with recent experimental measurement of edge conductance of relatively long samples ($\geq 3\mu\text{m}$) of HgTe-based quantum well [7]. Although we do not have sufficient information about the presence and properties of islands in the samples used in Ref. [7], it can be expected that the size of such islands is comparable to the size of the edge state of TI. For such islands, level spacing is sufficiently small, $\Delta \lesssim 1$ K. Hence, experimental observation of temperature-independent edge resistivity for temperatures in the interval $1 \text{ K} < T < 10 \text{ K}$ (see inset in Fig. 1a of [7]) is in good qualitative agreement with our theory.

ACKNOWLEDGMENTS

We thank I. V. Gornyi and V. S. Khrapai for useful discussions.

FUNDING

The work was carried out with financial support from the Russian Science Foundation (grant No. 25-12-00212), <https://rscf.ru/en/project/25-12-00212/>. The work of R.A. Niyazov was also partially supported by the Theoretical Physics and Mathematics Advancement Foundation “BASIS”.

CONFLICT OF INTEREST

The authors of this work declare that they have no conflicts of interest.

Appendix A: Scattering waves and field operators in the non-interacting case

In the non-interacting case, the scattering waves describing electrons moving from two leads read

$$\begin{aligned} |\psi_k^a\rangle &= \begin{cases} e^{ikx} |\uparrow\rangle, & x < 0, \\ [-f e^{iky} |\downarrow\rangle + r e^{ik(L-y)} |\uparrow\rangle] D(k), & 0 < y < L, \\ e^{ikx} e^{i\theta_k} |\uparrow\rangle, & x > 0, \end{cases} \\ |\psi_k^b\rangle &= \begin{cases} e^{-ikx} e^{i\theta_k} |\downarrow\rangle, & x < 0, \\ -[r e^{iky} |\downarrow\rangle + f e^{ik(L-y)} |\uparrow\rangle] D(k), & 0 < y < L, \\ e^{-ikx} |\downarrow\rangle, & x > 0. \end{cases} \end{aligned} \quad (\text{A1})$$

Here,

$$D(k) = \frac{1}{1 - t e^{ikL}}, \quad e^{i\theta_k} = (t - e^{ikL}) D(k), \quad (\text{A2})$$

and $|\uparrow\rangle$ and $|\downarrow\rangle$ are orthogonal spinors describing left- and right-moving edge states. Since we use basis of scattering waves, we can assume below that $k > 0$.

Annihilation field-operator $\hat{\Psi}$ in a certain coordinate point is given by

$$\hat{\Psi}(s) = \int \frac{dk}{2\pi} (\hat{c}_k^a |\psi_k^a\rangle + \hat{c}_k^b |\psi_k^b\rangle), \quad (\text{A3})$$

where $s = x$ inside the edge of the TI, $s = y$ in the edge of the island, and $\hat{c}_k^{a(b)}$ are the electron annihilation operators in the reservoirs $\mu_{a(b)}$.

Inside the puddle edge, for $s = y$, the field operator can be rewritten as follows

$$\hat{\Psi}(y) = \hat{\Psi}^R(y) |\downarrow\rangle + \hat{\Psi}^L(y) |\uparrow\rangle, \quad (\text{A4})$$

where

$$\begin{aligned} \hat{\Psi}^R(y) &= \int \frac{dk}{2\pi} e^{iky} (-f \hat{c}_k^a - r \hat{c}_k^b) D(k) \\ &= \int \frac{dk}{2\pi} e^{iky} D(k) \sqrt{r^2 + f^2} \hat{c}_k^R, \end{aligned} \quad (\text{A5})$$

is the “right” field operator,

$$\begin{aligned} \hat{\Psi}^L(y) &= \int \frac{dk}{2\pi} e^{ik(L-y)} (r \hat{c}_k^a - f \hat{c}_k^b) D(k) \\ &= \int \frac{dk}{2\pi} e^{ik(L-y)} D(k) \sqrt{r^2 + f^2} \hat{c}_k^L \end{aligned} \quad (\text{A6})$$

is the “left” field operator, and we introduced chiral annihilation operators

$$\begin{aligned} \hat{c}_k^R &= \frac{-f \hat{c}_k^a - r \hat{c}_k^b}{\sqrt{r^2 + f^2}}, \\ \hat{c}_k^L &= \frac{r \hat{c}_k^a - f \hat{c}_k^b}{\sqrt{r^2 + f^2}}, \end{aligned} \quad (\text{A7})$$

which obey standard commutation rules

$$\{\hat{c}_k^{R\dagger}, \hat{c}_{k'}^R\} = \{\hat{c}_k^{L\dagger}, \hat{c}_{k'}^L\} = 2\pi\delta(k - k'). \quad (\text{A8})$$

Using property

$$\int \frac{dk}{2\pi} e^{ik(y-y')} |D(k)|^2 (r^2 + f^2) = \delta(y - y'), \quad (\text{A9})$$

which is valid for $0 < y < L$ and $0 < y' < L$, we find that operators $\hat{\Psi}^{R,L}$ also have standard commutation rules

$$\{\hat{\Psi}^{R\dagger}(y), \hat{\Psi}^R(y')\} = \{\hat{\Psi}^{L\dagger}(y), \hat{\Psi}^L(y')\} = \delta(y - y'). \quad (\text{A10})$$

The densities of the right- and left-moving fermions are expressed in terms of these operators as follows:

$$\hat{n}_R = \hat{\Psi}^{R\dagger} \hat{\Psi}^R, \quad \hat{n}_L = \hat{\Psi}^{L\dagger} \hat{\Psi}^L. \quad (\text{A11})$$

Commuting operators $\hat{\Psi}^{R,L}$ with the total Hamiltonian $H_0 + H_{\text{int}}$ and using above equations, we arrive at equations for these operators in the Heisenberg representation:

$$\begin{aligned} i\hbar \frac{\partial \hat{\Psi}_R}{\partial t} &= v_F \hat{p} \hat{\Psi}_R + 2\pi\hbar v_F g \hat{n}_L \hat{\Psi}_R, \\ i\hbar \frac{\partial \hat{\Psi}_L}{\partial t} &= -v_F \hat{p} \hat{\Psi}_L + 2\pi\hbar v_F g \hat{n}_R \hat{\Psi}_L. \end{aligned} \quad (\text{A12})$$

Replacing now operators $\hat{n}_{R,L}$ with the corresponding quasiclassical densities, we find that Eqs. (A12) coincide with equations for particle moving in the time-dependent matrix potential acting in the island edge, for $0 < y < L$:

$$\hat{U}(y, t) = \begin{pmatrix} U_L(y - v_F t) & 0 \\ 0 & U_R(y + v_F t) \end{pmatrix}. \quad (\text{A13})$$

where

$$U_L = 2\pi g v_F n_R(y - v_F t), \quad U_R = 2\pi g v_F n_L(y + v_F t), \quad (\text{A14})$$

are periodic functions of y and, consequently, t , with the periods L and L/v_F , respectively. Expanding these functions in the Fourier series, we get

$$\hat{U}(y, t) = \sum_n \begin{pmatrix} U_{L,n} e^{iq_n(y - v_F t)} & 0 \\ 0 & U_{R,n} e^{iq_n(y + v_F t)} \end{pmatrix}, \quad (\text{A15})$$

where $q_n = 2\pi n/L$. The term with $n = 0$ corresponds to time-independent homogeneous potential acting at $0 < y < L$ given by Eq. (12) of the main text.

Appendix B: Zero-mode distribution function

Let us now derive Eqs. (23) and (24) of the main text. Since the total energy (24) is the sum of the “right” and “left” contributions, it is sufficient to derive corresponding expressions for the R-movers. To this end, we write

$$\begin{aligned} \hat{N}_R &= \int_0^L dy \hat{n}_R \\ &= \sum_{k,k'} \int_0^L dy D(k) D^*(k') e^{i(k-k')y} (1 - t^2) \hat{c}_{k'}^{R\dagger} \hat{c}_k^R, \end{aligned} \quad (\text{B1})$$

where $\sum_{k,k'} = \int dk dk' / (2\pi)^2$. The distribution function for N_R reads

$$f(N_R) = \left\langle \int \frac{d\varphi}{2\pi} \exp \left[i\varphi \left(N_R - \sum_{k,k'} A_{kk'} c_{k'}^{\text{R}\dagger} c_k^{\text{R}} \right) \right] \right\rangle_{\hat{\rho}}, \quad (\text{B2})$$

where matrix elements of the single-particle operator \hat{A} look

$$A_{kk'} = \int_0^L dy e^{i(k-k')y} (1-t^2) D(k) D^*(k'), \quad (\text{B3})$$

and averaging is taken over the equilibrium density matrix

$$\langle \dots \rangle_{\hat{\rho}} = \frac{\text{Tr}(\dots \hat{\rho})}{\text{Tr}(\hat{\rho})}, \quad (\text{B4})$$

$$\hat{\rho} = \exp[-(\hat{H}_0 - \mu)/T].$$

Here μ is the chemical potential in the leads. By using trace formula known in the full counting statistics theory (see [34] and Eq. (8) in [35]), we get

$$\left\langle \exp \left[-i\varphi \sum_{k,k'} A_{kk'} c_{k'}^{\text{R}\dagger} c_k^{\text{R}} \right] \right\rangle_{\hat{\rho}} = \det [1 - \hat{f} + \hat{f} e^{-i\varphi \hat{A}}]. \quad (\text{B5})$$

Here matrix elements of the operator \hat{f} read

$$f_{kk'} = f_F(k) 2\pi \delta(k - k'), \quad (\text{B6})$$

where $f_F(k) = f_F(E_k)$ is the Fermi distribution function. Using property Eq. (A9), one can check that all eigenvalues of operator \hat{A} equal to unity, so that Eq. (B5) is periodic function of φ with the period 2π , and, consequently, $f(N_R)$ is non-zero for integer values of N_R as it should be. In order to calculate $f(N_R)$ for $T \gg \Delta$, we write $\det[\dots] = \exp[\ln(\det[\dots])]$ and expand $\ln(\det[\dots])$ over φ up to the terms of the second order

$$\begin{aligned} & \ln [\det (1 - \hat{f} + \hat{f} e^{-i\varphi \hat{A}})] \\ & \approx \text{Tr} \left(-i\varphi \hat{f} \hat{A} - \frac{\varphi^2}{2} [\hat{f} \hat{A}^2 - (\hat{f} \hat{A})^2] \right) = -i\varphi \sum_k f_F(k) A_{kk} \\ & - \frac{\varphi^2}{2} \sum_{k,k'} f_F(k) [1 - f_F(k')] A_{kk'} A_{k'k} \approx -i\varphi N_0 \\ & - \frac{\varphi^2}{2} \sum_n f_F(k_n) [1 - f_F(k_n)] \approx -i\varphi N_0 - \frac{T}{\Delta} \frac{\varphi^2}{2}. \end{aligned} \quad (\text{B7})$$

Here, $N_0 = L \sum_k f_F(k)$, and $k_n = 2\pi n/L$. While obtaining two bottom lines in Eq. (B7), we took into account that $f_F(k)$ is a smooth function that does not change essentially on the scale $2\pi/L$, so that one can replace $|D(k)|^2 \rightarrow \langle |D(k)|^2 \rangle_k$, where averaging over k is taken over interval $2\pi/L$. Substituting Eq. (B7) into Eq. (B2), integrating over φ , and performing analogous calculations for the L-mover, we arrive at Eq. (23) of the main

text with energy $\epsilon_{N_R N_L}$ given by Eq. (24).

Appendix C: Scattering waves for the Hamiltonian $\hat{H}_0 + \hat{U}_0$.

The Hamiltonian $\hat{H}_0 + \hat{U}_0$ with boundary conditions imposed by scattering matrix Eq. (4) describes a single-particle time-independent problem. Solving corresponding Schrodinger equation, we find scattering states

$$\begin{aligned} |\psi_k^{\text{a}}\rangle &= \begin{cases} e^{ikx} |\uparrow\rangle + r_{\text{bs}} e^{-ikx} |\downarrow\rangle, & x < 0, \\ -f D(k_R) e^{ik_R y} |\downarrow\rangle + r D(k_L) e^{ik_L(L-y)} |\uparrow\rangle, & 0 < y < L, \\ Z_{\text{a}} e^{ikx} |\uparrow\rangle, & x > 0, \end{cases} \\ |\psi_k^{\text{b}}\rangle &= \begin{cases} Z_{\text{b}} e^{-ikx} |\downarrow\rangle, & x < 0, \\ -r D(k_R) e^{ik_R y} |\downarrow\rangle - f D(k_L) e^{ik_L(L-y)} |\uparrow\rangle, & 0 < y < L, \\ e^{-ikx} |\downarrow\rangle + r_{\text{bs}} e^{ikx} |\uparrow\rangle, & x > 0. \end{cases} \end{aligned} \quad (\text{C1})$$

Here,

$$\begin{aligned} k_R &= k - U_{L,0}/v_F, \\ k_L &= k - U_{R,0}/v_F, \\ U_{L,0} &= (2\pi g v_F/L) N_L, \\ U_{R,0} &= (2\pi g v_F/L) N_R, \\ r_{\text{bs}} &= f r [e^{ik_L L} D(k_L) - e^{ik_R L} D(k_R)], \\ Z_{\text{a}} &= t - r^2 e^{ik_L L} D(k_L) - f^2 e^{ik_R L} D(k_R), \\ Z_{\text{b}} &= t - r^2 e^{ik_R L} D(k_R) - f^2 e^{ik_L L} D(k_L), \end{aligned} \quad (\text{C2})$$

and $D(k)$ is given by Eq. (A2)

Appendix D: Effect of the dynamical part of the interaction

Let us now consider effect of the dynamical part of the potential Eq. (11)

$$\hat{U}'(y, t) = \sum_{n \neq 0} \begin{pmatrix} U_{L,n} e^{iq_n(y+v_F t)} & 0 \\ 0 & U_{R,n} e^{iq_n(y-v_F t)} \end{pmatrix}. \quad (\text{D1})$$

We expand wave function over non-interacting scattering states, Eq. (A1):

$$\Psi = \sum_k (c_k^{\text{a}} |\psi_k^{\text{a}}\rangle + c_k^{\text{b}} |\psi_k^{\text{b}}\rangle) e^{-iEt}, \quad (\text{D2})$$

where coefficients $c_k^{\text{a,b}}$ obey

$$i\dot{c}_k^{\alpha} = \sum_{k',\beta} V_{kk'}^{\alpha\beta}(t) c_{k'}^{\beta} e^{i(E_k - E_{k'})t}. \quad (\text{D3})$$

Here $V_{kk'}^{\alpha\beta}(t)$ is time-dependent matrix element of the potential U' corresponding to transition from k', β to k, α . Direct calculation yields the following expressions

$$\begin{aligned}
V_{k,k'}^{a,b} e^{i(E_k - E_{k'})t} &= fr \sum_{n \neq 0} \frac{e^{i(k' - k)L} - 1}{i(k' - k + q_n)} e^{iv_F t(q_n + k - k')} (U_{R,n} - U_{L,-n}) D(k') D^*(k), \\
V_{k,k'}^{b,b} e^{i(E_k - E_{k'})t} &= \sum_{n \neq 0} \frac{e^{i(k' - k)L} - 1}{i(k' - k + q_n)} e^{iv_F t(q_n + k - k')} (f^2 U_{L,-n} + r^2 U_{R,n}) D(k') D^*(k), \\
V_{k,k'}^{a,a} e^{i(E_k - E_{k'})t} &= V_{k,k'}^{b,b} e^{i(E_k - E_{k'})t} \Big|_{r \leftrightarrow f}
\end{aligned} \tag{D4}$$

Let us find probabilities of transition per unit time from k' to k caused by n -th harmonics of the dynamical potential, $W_{k,k'}^{a,b}(n)$ and $W_{k,k'}^{b,b}(n)$. Integrating above matrix elements over time from zero to t and squaring the resulting expressions, we obtain the standard golden-rule delta-function $\delta[v_F(q_n + k - k')]$. Hence, $k' = k + q_n$. Then, factor standing in front of delta-function turns to zero:

$$\left| \frac{e^{i(k' - k)L} - 1}{i(k' - k + q_n)} \right|^2 \rightarrow 0, \quad \text{for } k' = k + q_n. \tag{D5}$$

Hence,

$$W_{k,k'}^{a,b}(n) = W_{k,k'}^{b,b}(n) = 0. \tag{D6}$$

This result justifies the neglect of the dynamical part of the Hamiltonian.

-
- [1] B. A. Bernevig and S.-C. Zhang, Phys. Rev. Lett. **96**, 106802 (2006).
 - [2] B. A. Bernevig, T. L. Hughes, and S.-C. Zhang, Science **314**, 1757 (2006).
 - [3] C. L. Kane and E. J. Mele, Phys. Rev. Lett. **95**, 146802 (2005).
 - [4] M. König, S. Wiedmann, C. Brüne, A. Roth, H. Buhmann, L. W. Molenkamp, X.-L. Qi, and S.-C. Zhang, Science **318**, 766 (2007).
 - [5] M. König, M. Baenninger, A. G. F. Garcia, N. Harjee, B. L. Pruitt, C. Ames, P. Leubner, C. Brüne, H. Buhmann, L. W. Molenkamp, and D. Goldhaber-Gordon, Phys. Rev. X **3**, 021003 (2013).
 - [6] G. Gusev, Z. Kvon, E. Olshanetsky, and N. Mikhailov, Solid State Communications **302**, 113701 (2019).
 - [7] E. Olshanetsky, Z. Kvon, G. Gusev, and N. Mikhailov, Physica E: Low-dimensional Systems and Nanostructures **147**, 115605 (2023).
 - [8] Y. Tanaka, A. Furusaki, and K. A. Matveev, Phys. Rev. Lett. **106**, 236402 (2011).
 - [9] J. Maciejko, C. Liu, Y. Oreg, X.-L. Qi, C. Wu, and S.-C. Zhang, Phys. Rev. Lett. **102**, 256803 (2009).
 - [10] V. Cheianov and L. I. Glazman, Phys. Rev. Lett. **110**, 206803 (2013).
 - [11] M. V. Durnev and S. A. Tarasenko, Phys. Rev. B **93**, 075434 (2016).
 - [12] P. D. Kurilovich, V. D. Kurilovich, I. S. Burmistrov, Y. Gefen, and M. Goldstein, Phys. Rev. Lett. **123**, 056803 (2019).
 - [13] T. L. Schmidt, S. Rachel, F. von Oppen, and L. I. Glazman, Phys. Rev. Lett. **108**, 156402 (2012).
 - [14] J. I. Vayrynen, M. Goldstein, and L. I. Glazman, Phys. Rev. Lett. **110**, 216402 (2013).
 - [15] J. I. Vayrynen, M. Goldstein, Y. Gefen, and L. I. Glazman, Phys. Rev. B **90**, 115309 (2014).
 - [16] V. A. Sablikov, Phys. Rev. B **102**, 075434 (2020).
 - [17] P. P. Aseev and K. E. Nagaev, Phys. Rev. B **94**, 045425 (2016).
 - [18] H. Maier, J. Ziegler, R. Fischer, D. Kozlov, Z. D. Kvon, N. Mikhailov, S. A. Dvoretzky, and D. Weiss, Nature Communications **8**, 2023 (2017).
 - [19] J. Ziegler, *Quantum transport in HgTe topological insulator nanostructures*, Ph.D. thesis, University of Regensburg, Regensburg (2019).
 - [20] P. Delplace, J. Li, and M. Büttiker, Phys. Rev. Lett. **109**, 246803 (2012).
 - [21] R. A. Niyazov, D. N. Aristov, and V. Y. Kachorovskii, Phys. Rev. B **108**, 075424 (2023).
 - [22] J. C. Y. Teo and C. L. Kane, Phys. Rev. B **79**, 235321 (2009).
 - [23] A. P. Dmitriev, I. V. Gornyi, V. Y. Kachorovskii, and D. G. Polyakov, Phys. Rev. Lett. **105**, 036402 (2010).
 - [24] A. P. Dmitriev, I. V. Gornyi, V. Y. Kachorovskii, D. G. Polyakov, and P. M. Shmakov, JETP Letters **100**, 839 (2015).
 - [25] A. P. Dmitriev, I. V. Gornyi, V. Y. Kachorovskii, and D. G. Polyakov, Phys. Rev. B **96**, 115417 (2017).
 - [26] T. Giamarchi, *Quantum Physics in One Dimension*, The international series of monographs on physics, Vol. 121 (Clarendon; Oxford University Press, 2004).
 - [27] R. A. Niyazov, I. V. Krainov, D. N. Aristov, and V. Y. Kachorovskii, "A mechanism of strong backscattering in helical edge states," the paper is being prepared for publication.
 - [28] F. D. M. Haldane, J. Phys. C Solid State Phys. **14**, 2585 (1981).
 - [29] D. Loss, Phys. Rev. Lett. **69**, 343 (1992).
 - [30] Y. M. Galperin, B. L. Altshuler, J. Bergli, and D. V. Shantsev, Phys. Rev. Lett. **96**, 097009 (2006).
 - [31] J. Schrieffer, Y. Makhlin, A. Shnirman, and G. Schön, New J. Phys. **8**, 1 (2006).
 - [32] C. Neuenhahn, B. Kubala, B. Abel, and F. Marquardt,

- Phys. Status Solidi B **246**, 1018 (2009).
- [33] D. N. Aristov and R. A. Niyazov, Phys. Rev. B **94**, 035429 (2016).
- [34] L. S. Levitov, H. Lee, and G. B. Lesovik, J. Math. Phys. **37**, 4845 (1996).
- [35] I. Klich, in *Quantum Noise in Mesoscopic Physics*, NATO Science Series, Vol. 97, edited by Y. Nazarov (Springer Science & Business Media, Dordrecht, 2003) pp. 397–402.